19th Brazilian Congress of Thermal Sciences and Engineering
November 6th–10th, 2022, Bento Gonçalves - RS - Brazil

Stability Approach for Automotive Fuel Tank System Premature Shutt-Off Prediction

Eric Neugebauer
Karl Peter Burr
Universidade Federal do ABC
neugebauer.eric@yahoo.com, karl.burr@ufabc.edu.br

Abstract.
Almost every driver had the experience of fuel pump shutdown before the car fuel tank is completely filled up, the premature shut-off. This phenomenon is a source of automobile industry customer dissatisfaction. According to the literature, the normal filling process has three phases: an initial transient phase; a second phase when pressure is constant in time along the tank system; and a short final transient phase before the fuel pump stops.
The objective of this work is to explain premature shut off as a consequence of the absence of the system pressure steady state (second phase) in the fuel supply process using an adequate flow model and linear stability analysis.
The solution corresponding to the second phase of the fuel supply process is constructed numerically as a function of the system parameters and boundary conditions space (SPBC space) and its linear stability is studied. This solution is denoted as an almost stationary (AS) state since it is an explicit linear function of time. The linearized governing equations with respect to the AS state gives a linear nonautonomous system of algebraic differential equations (DAE) and standard linear stability techniques do not apply. The finite time (less than the fill up time) action of this linear DAE system over a unitary volume in the phase space dictates the AS state linear stability. Stability maps in the SPBC space are obtained.

Keywords: *automotive fuel tank system, fuel supply premature shutt-off, multi-phase flow, linear stability analysis, nonautonomous dynamic systems*

1. INTRODUCTION

Premature shut-off of the fuel pump before the vehicle tank is completely filled up is a primary source of customer dissatisfaction and is still of main concern for the automotive industry.

Figure 1 below illustrate the tank pressure variation for a normal fuel supply process. Phase I indicates the initial transient in the fuel supply process. It starts with the opening of the fuel supply pipe and tank pressure equalization with the atmosphere. As the fuel starts filling in the tank, the pressure in the tank rises to make the gas inside the tank to flow out to the atmosphere. After this initial transient, the tank pressure stabilizes and an almost steady state regime is established, which is the phase II of the fuel supply process. Phase II is an almost steady state since all dependents variables remain constant except for the tank liquid depth which varies linearly with time. Finally, phase III sets in when the tank pressure rises and the gas-liquid mixture level in the filler tube or the liquid level in the vent tube reaches the fuel nozzle sensor, which shutsdown the fuel supply process.

According to Godbille *et al.* (2007) and in Fackrell *et al.* (2003), the fuel supply process can go wrong in different ways, which are the spill back and the premature shut-off. The spill back occurs when fuel drops flow away from the pipe entrance or when slugs of liquid come off the pipe entrance. Spill back phenomenum poses a problem for the fuel supply operator, but premature shut-off does not. It only causes customer dissatisfaction since the tank is just partially filled up. The supply process when premature shut-off occurs is similar to the normal supply process, however the rise of the gas-liquid mixture level in the filler tube seen in phase III of the normal fuel supply process happens before the tank is filled up.

The absense of phase II of the normal fuel supply process with large enough rise of the gas-liquid mixture level in the filler tube during the initial transient (phase I) of the fuel supply process to cause the fuel pump shutdown is the main hypothesis in this work for premature shut-off to occur. This hypothesis is investigated through linear stability analysis. The almost steady state solution which represents phase II of the normal fuel supply process can be seen as a stable

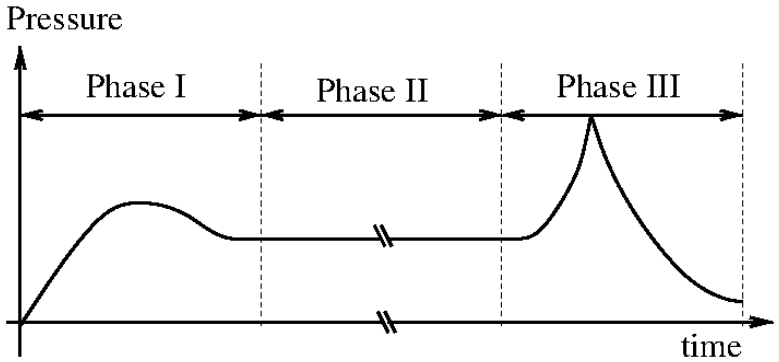

Figure 1: Tank pressure evolution during normal fuel supply process (source Fackrell *et al.* (2003))

almost stationary state of an adequate mathematical flow model for the two-phase flow in the fuel tank system. If the almost stationary state solution which represents the phase II looses stability, phase II of the fuel supply process will not exists, what may open the possibility for premature shut-off to occur.

According to Mastroianni *et al.* (2011), the premature shut off may be caused by many factors, just as poor pipe geometry design, sharp pipe curvature near the pipe inlet, pipe diameter restrictions and safety valve and auxiliary ventilation pipe geometry.

Computational fluid dynamics was used by many authors to simulate the two-phase flow in fuel tank systems. Examples of this line of research are Sinha *et al.* (1998), Banerjee *et al.* (2002), Banerjee *et al.* (2001), Dutra *et al.* (2011) and Buscariolo *et al.* (2015). Experimental results in the literature are limited. Basically, Mastroianni *et al.* (2011) studied experimentally the influence of the diameter of the auxiliary duct, of the fuel vaporization rate and of the fuel flow rate in the occurrence of premature shut off.

For the analysis proposed in this work, computational fluid dynamics models are not adequate since they lead to very large systems of equations which implies in huge computational costs. A more simple model is needed and a simplified version of the model presented in Fackrell *et al.* (2003) is addopted in this work. The vehicle fuel tank system in Fackrell *et al.* (2003) is modeled as a series of four control volumes and four valves. The liquid is assumed incompressible, fuel vaporization is taken into account and temperature is assumed constant. Mastroianni *et al.* (2011) compared experimental results with simulation of Fackrell *et al.* (2003) model. The simulation results agreed well with experiments of normal fuel supply process. It also gave reasonable prediction for premature shut off, but not for all experimental situations where premature shut off happened.

In the next section, the simplified version of the model presented in Fackrell *et al.* (2003) is described. In the third section, linear stability analysis of the almost stationary state of the model described in the previous section is performed and a stability criterion is given. Results for the As state and a stability maps in the system parameter space are given in the fourth section and a discussion and conclusions are presented in the fifth section.

2. Fuel Tank Two-Phase Flow Model

The vehicle fuel tank system is composed of many parts, where the most commons are the fuel tank, the pipe connecting the pump nozzle to the tank, the auxiliary ventilation duct and a safety valve to avoid fuel leakage in the case of an accident (see Fackrell *et al.* (2003) for an illustration of a vehicle fuel tank system).

The model presented in Fackrell *et al.* (2003) is considered in this work, but the formation of fuel vapour is neglected. This assumption leads to a smaller and more simple set of governing equations for the two-phase flow in the fuel tank system. Fackrell *et al.* (2003) consider a constant value for the void fraction, but in this work the void fraction is a function of time and given by a drift-flux model. The liquid is assumed incompressible, the gas is considered as an ideal gas and the temperature is assumed constant. The fuel tank system is modelled as four control volumes and three valves, as illustrated in Fig. 2. Mass conservation is considered for each control volume and each valve, but energy conservation is appied to each valve only. To obtain one more equation for control volumes one and two, a force balance among pressure, friction and gravitational forces is considered, but inertia forces are discarded. The result is a system of algebraic-differential equations.

Control volume 1 (CV1) represents the annular area of the filler tube around the liquid that flows from the nozzle and is aproximated as a liquid column with diameter assumed equal to the nozzle diameter (see Fig. 2). Pressure change in CV1 is due to the gas flow 1) from the vent tube connected to the tank, 2) through the openning around the nozzle and 3) into the control volume 2. It is also affected by the movement of the interface between control volumes 1 and 2. Mass conservation for the control volume 1 leads to

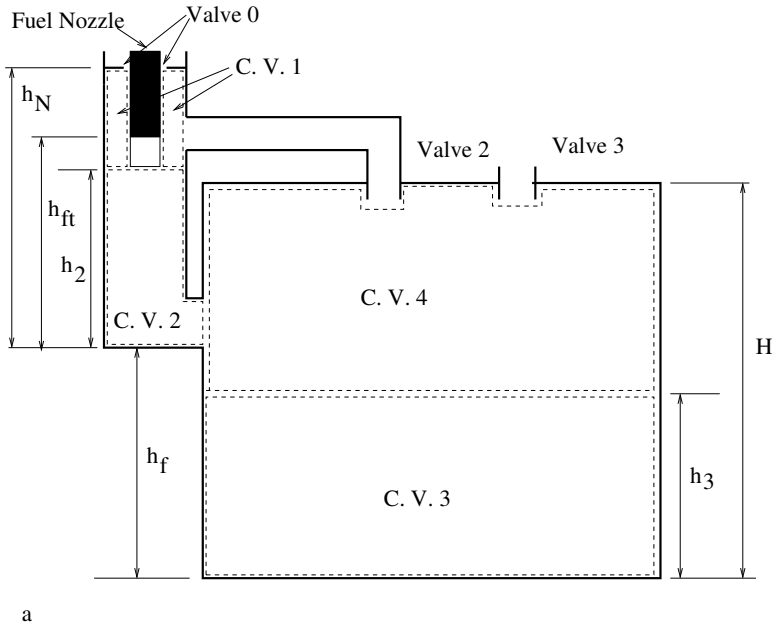

Figure 2: Schematic diagram of a simple fuel tank system showing the four control volumes and the three valves.

$$\frac{dP_1}{dt} - \frac{P_1}{h_n - h_2}\frac{dh_2}{dt} = \frac{RT}{(A_2 - A_n)(h_n - h_2)}\left[\frac{P_4 Q_{4-1}}{RT} + \frac{P_1}{RT}A_{v_0}V_{v_0} - \frac{P_1}{RT}Q_g\right], \tag{1}$$

where P_1 is the pressure in CV1, R is the gas constant, T is the temperature, h_N is the height of the nozzle from the filler tube bottom, h_2 is the height of gas-liquid mixture in the filler tube (also the height of control volume 2), A_2 is the cross-sectional area of the filler tube, A_N is the cross-sectional area of the nozzle, Q_l is the volume flow rate of liquid fuel from the dispensing nozzle, Q_g is the gas volumetric flow rate from CV1 into control volume 2 (CV2), A_{V_0} is the cross-sectional area of the space between the nozzle and the openning of the filler tube, V_{V_0} is the fluid velocity through A_{V_0}, P_4 is the pressure in control volume 4 (CV4) and Q_{l4-1} is the volumetric flow rate of fluid between CV4 and CV1.

With the rise in the tank pressure in the early stage of the fuel supply process, the fluid flow out of the filler tube slows while the fuel flow into the filler tube remains constant. As a consequence, fluid collects in the filler tube. This fluid collection is contained in control volume 2 (CV2) and is a gas-liquid mixture with void fraction α. Mass conservation of the two-phase flow in CV2 leads to

$$\bar{\rho}_2\frac{dh_2}{dt} + h_2\frac{d\bar{\rho}_2}{dt} = \frac{\bar{\rho}_2}{A_2}\left(Q_l + Q_g - Q_{2-3}\right), \tag{2}$$

where Q_{2-3} is the volumetric flow rate of the gas-liquid mixture flowing from the filler tube into the tank. $\bar{\rho}_2$ is the liquid-gas mixture density given by the equation

$$\bar{\rho}_2 = \rho_l(1-\alpha) + \frac{P_1}{RT}\alpha, \tag{3}$$

where it is assumed that the gas pressure in CV2 can be approximated by the gas presure in CV1.

After the fluid reaches the tank, it is assumed that the liquid and gas separates with the liquid falling to the bottom and the gas rising to the top part of the tank. Control volume 3 (CV3) contains the collection of liquid fuel in the tank. Mass conservation to CV3 leads to

$$\frac{dh_3}{dt} = \frac{1}{A_3}(1-\alpha)\,Q_{2-3}, \tag{4}$$

where h_3 is the liquid depth in the tank and A_3 is the tank cross-sectional area.

Control volume 4 (CV4) represents the gas (air) that is collected in the tank only, since it is assumed that there is no fuel vaporization in the present model. The source of gas to the tank is through the filler tube and the exit ports for the

gas in the tank are the rollover valve and the vent tube connected to the filler tube (see Fig. 2). Mass conservation for the fluid in CV4 leads to

$$\frac{dP_4}{dt} - \frac{P_4}{(H-h_3)}\frac{dh_3}{dt} = \frac{\alpha P_1 Q_{2-3}}{A_4\,(H-h_3)} - \frac{P_4}{A_4\,(H-h_3)}\left(Q_{4-1} + A_{v_3}V_{v_3}\right), \tag{5}$$

where H is the tank height, A_4 is the CV4 cross-sectional area, A_{V_3} is the cross-sectional area of valve 3 (roll over valve) and V_{V_3} is the fluid velocity in valve 3.

The flow through the valves is assumed one-dimensional and there is no heat transfer. Mass and energy conservation are applied to each valve.

Valve 0 (see Fig. 2 for its location) is the space between the dispensing nozzle and the filler tube. Mass and energy conservation leads to the valve 0 governing equation

$$V_{V_0}^2 = \begin{cases} \frac{P_{atm}-P_1}{P_1}\frac{2RT}{\left(\frac{f_{V_0}L_{V_0}}{D_{V_0}}+K_{ent}+K_{exit}\right)} & \text{if } P_{atm} \geq P_1, \\ \frac{P_1-P_{atm}}{P_1}\frac{2RT}{\left(\frac{f_{V_0}L_{V_0}}{D_{V_0}}+K_{ent}+K_{exit}\right)} & \text{if } P_{atm} < P_1, \end{cases} \tag{6}$$

where f_{V_0} is the Darcy-Weisbach friction factor for valve 0, L_{V_0} is the effective length of valve 0, D_{V_0} is the effective diameter of valve 0, K_{ent} is the valve 0 entrance loss coefficient and K_{exit} is the valve 0 exit loss coefficient. The Darcy-Weisbach friction factor is four time the fanning friction factor, which is a function of the flow Reynolds number and pipe wall roughness ε. It is given by the equation

$$f(Re,\epsilon/D) = \begin{cases} f_{lam} = \frac{16}{Re} & \text{for } Re \leq 2000 \\ f_{turb} = \left\{-4\log_{10}\left(\frac{1}{3{,}7065}\frac{\epsilon}{D}\right.\right. & \\ \left.\left. -\frac{5{,}0452}{Re}\log_{10}\left[\frac{1}{2{,}8257}\left(\frac{\epsilon}{D}\right)^{1{,}1098}+\frac{5{,}8506}{Re^{0{,}8981}}\right]\right)\right\}^{-2} & \text{for } Re \geq 2300 \\ \frac{f_{lam}(2000;\epsilon/D)(2300-Re)+f_{turb}(2300;\epsilon/D)(Re-2000)}{300} & \text{for } 2000 < Re < 2300 \end{cases}. \tag{7}$$

It is assumed that the valves wall and pipes wall have no roughness ($\varepsilon = 0$). An additional governing equation for the top part of the filler tube, which is CV1, is obtained considering a force balance equation among the pressure, friction and gravitational forces in CV1. The flow losses in CV1 due to turbulence caused by the flow entrance in CV1 from valve 0 and from the auxiliary tube are accounted for through the use of the concept of equivalent pipe length to emulate the loss due to flow turbulence. This force balance results in the equation

$$\begin{array}{ll} -\frac{1}{2}\pi\frac{P_1}{RT}\left\{[D_1(h_N-h_2+Le_1D_1)+D_N(h_N-h_{ft})]f_g(Re_g,\epsilon/D_1)\frac{Q_g}{A_1}\left|\frac{Q_g}{A_1}\right|\right. & \\ \left. -D_N(h_{ft}-h_2)f_i(Re_i,\epsilon/D_N)\left(\frac{Q_g}{A_1}-\frac{Q_l}{A_N}\right)\left|\frac{Q_g}{A_1}-\frac{Q_l}{A_N}\right|\right\} + \frac{P_1}{RT}gA_1(h_N-h_2) = 0 & \text{for } h_2 \leq h_{ft}, \\ -\frac{1}{2}\pi\frac{P_1}{RT}\left\{[D_1(h_N-h_2+Le_1D_1)+D_N(h_N-h_2)]f_g(Re_g,\epsilon/D_1)\frac{Q_g}{A_1}\left|\frac{Q_g}{A_1}\right|\right\} & \\ +\frac{P_1}{RT}gA_1(h_N-h_2) = 0 & \text{for } h_2 > h_{ft}, \end{array} \tag{8}$$

where g is the gravity acceleration constant, $f_g = f(Re_g,\epsilon/D)(f_i = f(Re_i,\epsilon/D_N))$ is the gas-pipe wall (gas-liquid jet interface) friction factor, D_1 is the filler tube diameter, A_N is the nozzle and liquid jet cross sectional area, $A_1 = A_2 - A_N$ is the cross sectional area of the annular region between the filler tube wall and the nozzle wall or liquid jet boundary. A_2 is the filler tube cross sectional area. Le_1 is the equivalent pipe length to emulate the loss due to flow turbulence and its value can be obtained from table 4.1 of reference Govier (2008). The gas-pipe wall interface friction factor is a function of the gas Reynods number Re_g, given by the equation

$$Re_g = \frac{P_1 D_1 |Q_g|}{A_1 RT\mu_g}, \tag{9}$$

and the gas-liquid jet interface friction factor f_i is a function of the gas-liquid jet interface Reynolds number Re_i, given by the equation

$$Re_i = \frac{P_1 D_N}{RT\mu_g}\left|\frac{Q_g}{A_1}-\frac{Q_l}{A_N}\right|, \tag{10}$$

where μ_g is the gas dynamic viscosity. For CV2, and additional equation can be obtained through a force balance among pressure, friction and gravitacional forces. Inertial forces are neglected. This results in the equation

$$\begin{aligned} P_1 - P_4 - \bar{\rho}_2 \left\{ \frac{2}{D_1} f_m(Re_m, \epsilon/D) \frac{Q_{2-3}}{A_2} \left| \frac{Q_{2-3}}{A_2} \right| (h_2 + Le_2 D_1) - g h_2 \right\} = 0 \quad & \text{for } h_3 \leq h_f \\ P_1 - P_4 - \rho_l g (h_3 - h_f) - \bar{\rho}_2 \left\{ \frac{2}{D_1} f_m(Re_m, \epsilon/D) \frac{Q_{2-3}}{A_2} \left| \frac{Q_{2-3}}{A_2} \right| (h_2 + Le_2 D_1) - g h_2 \right\} = 0 \quad & \text{for } h_3 > h_f \end{aligned} \tag{11}$$

where h_f is the filler tube bottom height with respect to the tank bottom, $\bar{\rho}_2$ is the gas-liquid mixture density in CV2 and is given by Eq. (3), Le_2 is the equivalent pipe length to emulate the losses due to the filler tube connection to the tank. This connection was considered as an elbow and the equivalent pipe length for this pipe feature is given in table 4.1 of Govier (2008). $f_m(Re_m, \epsilon/D) = f(Re_m, \varepsilon/D_1)$ is the gas-liquid mixture pipe wall friction factor, which is a function of the mixture Reynolds number Re_m given by the equation

$$Re_m = \frac{\bar{\rho}_2 D_2 |Q_g|}{A_2[(1-\alpha)\mu_l + \alpha \mu_g]} \tag{12}$$

where μ_l is the liquid dynamics viscosity.

Valve 2 models the ventilation tube and the ventilation tube valve. If mass and energy conservation are applied between the ventilation tube valve entrance in the tank and the exit of the ventilation tube at the filler tube, the resulting equation is

$$Q_{4-1}^2 = \frac{P_4 - P_1}{P_4} \frac{RT}{\frac{1}{2(A_{V_T})^2} - \frac{1}{2(A_{V_2})^2} + \left(\frac{f_{V_2} L_{V_2}}{D_{v_2}} + K_L + K_{reent} \right) \frac{1}{2(A_{V_2})^2} + \left(\frac{f_{V_T} L_{V_T}}{D_{V_T}} + K_{exit} \right) \frac{1}{2(A_{V_T})^2}}, \tag{13}$$

where f_{V_2} is the friction factor for the vent tube and valve ($f_{V_T} = f_{V_2}$), L_{V_2} is the effective length of the vent tube valve, D_{V_2} is the diameter of the vent tube valve, K_L is the transition loss coefficient, K_{reent} is the reentrance loss coefficient, L_{V_T} is the effective length of the tube connecting the vent tube valve to the filler tube and D_{V_T} is the diameter of the connecting tube.

Valve 3 accounts for the flow losses at the rollover valve. Mass conservation and energy conservation between the entrance and exit of the rollover valve leads to

$$V_{v_3}^2 = \left[\frac{P_4 - P_{atm}}{P_4} \right] \frac{2RT}{\left(\frac{f_{v_3} L_{v_3}}{D_{v_3}} + K_{ent} + K_{exit} \right)}, \tag{14}$$

where f_{V_3} is the friction factor for the rollover valve, L_{V_3} is the effective length of the rollover valve and D_{V_3} is the diameter of the rollover valve.

To close the model a drift-flux relation to determine the value of the void fraction α is addopted. The drift-flux relation can be writen in the form

$$\alpha \left[A_2 U_D + C_D (Q_l + Q_g) \right] - Q_g = 0, \tag{15}$$

where U_D is the drift velocity and C_D is the distribution parameter. In the filler tube the flow is in general a cocurrent downward two-phase flow, but counter-current flow maybe possible for large liquid volumetric flow rates before flooding happens. For cocurrent downward two-phase flow the drift velocity and the distribution parameter are in general dependent on the flow regime, but flow regime transition criteria for downward two-phase flow in a vertical channel, like the filler tube, have not been well developed according to Lokanathan and Hibiki (2018). Therefore, the distributio parameter C_D and the drift velocity U_D for cocurrent downflow are given by the Chexal-Lellouche correlation, which is independent of the flow pattern, applicable to a full range of thermodynamic conditions and geometries, and covers air-water counter-current flows. The Chexal-Lellouche correlation can be found in Hibiki (2019), Chexal *et al.* (1997) and Chexal *et al.* (1992).

The mathematical model for the two-phase flow in the fuel tank system is composed by Eqs. (1)-(6) and (8)-(15) with dependent variables $P_1, P_4, h_2, h_3, \bar{\rho}_2, Q_g, Q_{2-3}, Q_{4-1}, V_{V_0}, V_{v_3}$ and α. Equations (1)-(2) and (4)-(5) are ordinary differential equations, but Eqs. (3) and (6)-(15) are algebraic equations. Therefore, the mathematical flow model is a system of algebraic-differential equations (DAE). This set of equations can be written in matrix form as

$$\begin{aligned} \mathbf{M}(\mathbf{y}(t)) \frac{d}{dt} \mathbf{y}(t) &= \mathbf{F}(\mathbf{y}(t), \mathbf{z}(t)) \\ \mathbf{0} &= \mathbf{G}(\mathbf{y}(t), \mathbf{z}(t)) \end{aligned} \tag{16}$$

where $\mathbf{y}(t) = \{P_1\ P_4\ h_2\ h_3\ \bar{\rho}_2\}^T, \mathbf{z}(t) = \{\alpha\ Q_g\ Q_{2-3}\ Q_{4-1}\ V_{V_0}\ V_{v_3}\}^T$, the lines of vector $\mathbf{F}(\mathbf{y}(t), \mathbf{z}(t))$ corresponds to the right hand side of Eqs. (1), (2), (4) and (5), and the lines of vector $\mathbf{G}(\mathbf{y}(t), \mathbf{z}(t))$ corresponds to the algrabraic Eqs. (3), (6) and (8)-(15).

2.1 Differential Index Analysis

The DAE system, given by Eq. (16), is not in the semi-explicit form since matrix $\mathbf{M}$ is not a square matrix with non-zero elements only in the main diagonal. There are four differential equations involving time differentials of five dependent variables.

To determine the differential index of the DAE system given by Eq. (16), the algebraic part of the DAE system should be differentiated with respect to time as many times as necessary to obtain equations enough to express the first order derivatives of each dependent variable with respect to time in terms of the dependent variables. In the case of the DAE system given by Eq. (16), one time diferentiation of each algebric equation is enough to expresse the time derivative of each dependent variable in terms of dependent variables. If the algebraic Eqs. (3), (6), (8), (11), (13), (14) and (15) are examined, the dependent variable Q_{2-3} appears only in the Eq. (11) and the variable V_{V_3} appears only in the Eq. (14). Therefore, these two equations are used to write dQ_{2-3}/dt and dV_{V_3}/dt in terms of the dependent variables if $\frac{\partial G_4}{\partial Q_{2-3}} \neq 0$ and $\frac{\partial G_6}{\partial V_{V_3}} \neq 0$. To express the time derivative of the other dependent variables in terms of dependent variables, consider the ODEs in Eq. (16) and the time derivative of the first, second, thrid, fifth and seventh algebraic relations, which results in the following set of ODEs

$$\mathbf{K}\frac{d}{dt}\mathbf{w} = \mathbf{B},\ \text{with}\ \mathbf{K} = \begin{bmatrix} 1 & 0 & -\frac{P_1}{h_N - h_2} & 0 & 0 & 0 & 0 & 0 & 0 \\ 0 & 0 & \bar{\rho}_2 & 0 & h_2 & 0 & 0 & 0 & 0 \\ 0 & 0 & 0 & 1 & 0 & 0 & 0 & 0 & 0 \\ 0 & 1 & 0 & -\frac{-P_4}{H - h_3} & 0 & 0 & 0 & 0 & 0 \\ \frac{\partial G_1}{\partial P_1} & 0 & 0 & 0 & \frac{\partial G_1}{\partial \bar{\rho}_2} & 0 & 0 & 0 & \frac{\partial G_1}{\partial \alpha} \\ \frac{\partial G_2}{\partial P_1} & 0 & 0 & 0 & 0 & 0 & 0 & \frac{\partial G_2}{\partial V_{V_0}} & 0 \\ 0 & 0 & \frac{\partial G_3}{\partial h_2} & 0 & 0 & \frac{\partial G_3}{\partial Q_g} & \frac{\partial G_3}{\partial Q_{4-1}} & \frac{\partial G_3}{\partial V_{V_0}} & 0 \\ \frac{\partial G_5}{\partial P_1} & \frac{\partial G_5}{\partial P_4} & 0 & 0 & 0 & 0 & \frac{\partial G_5}{\partial Q_{4-1}} & 0 & 0 \\ \frac{\partial G_7}{\partial P_1} & 0 & 0 & 0 & 0 & \frac{\partial G_7}{\partial Q_g} & 0 & 0 & \frac{\partial G_7}{\partial \alpha} \end{bmatrix}, \tag{17}$$

with vector $\mathbf{w}^T = \{P_1\ P_4\ h_2\ h_3\ \bar{\rho}_2\ Q_g\ Q_{4-1}\ V_{V_0}\}$ and with vector $\mathbf{B}^T = \{F_1\ F_2\ F_3\ F_4\ 0\ 0\ 0\ 0\ 0\}$. The system of ODEs, given by Eq. (17), can be solved for $\frac{d}{dt}\mathbf{w}$ if and only if

$$\det\{\mathbf{K}\} \neq 0 \tag{18}$$

If this condition and the conditions $\frac{\partial G_4}{\partial Q_{2-3}} \neq 0$ and $\frac{\partial G_6}{\partial V_{V_3}} \neq 0$ are satisfied, the DAE system given by Eq. (16) has differential index one. These conditions can be checked numerically during time integration of the Eq. (16).

2.2 Simplified Flow Model

To obtain a model governed by a DAE in semi-explicit form, we assume the void fraction α constant and with its value equal to the almost stationary state void fraction. With this assumption, $\bar{\rho}_2$ is only a function of the pressure P_1 and the differential part of the DAE system, given by Eq. (16), can now be written in semi-explicit form as

$$\frac{dP_1}{dt} = -\frac{\bar{\rho}_2 RT}{\bar{\rho}_2 RT(h_N - h_2) + P_1 \alpha h_2}\left\{\frac{P_1}{A_3}(Q_l + Q_g - Q_{2-3}) + \frac{1}{A_2 - A_N}(P_4 Q_{4-1} + P_1 A_{v_0} V_{V_0} - P_1 Q_g)\right\} \tag{19}$$

$$\frac{dP_4}{dt} = \frac{1}{A_4(H - h_3)}\left\{P_4(1-\alpha)Q_{2-3} + P_1 \alpha Q_{2-3} - P_4\left[Q_{4-1} + A_{V_3} V_{V_3}\right]\right\} \tag{20}$$

$$\frac{dh_2}{dt} = -\frac{h_2 \alpha}{\bar{\rho}_2 RT(h_N - h_2) + P_1 \alpha h_2}\left\{\frac{P_1}{A_3}(Q_l + Q_g - Q_{2-3}) + \frac{1}{A_2 - A_N}(P_4 Q_{4-1} + P_1 A_{v_0} V_{V_0} - P_1 Q_g)\right\} + \frac{1}{A_3}(Q_l + Q_g - Q_{2-3}) \tag{21}$$

and the fourth differential equation is given by Eq. (4). The algebraic part of the simplified DAE system is given by Eqs. (6), (8), (11), (13) and (14). The simplified model system of equations can be written in matrix form as

$$\begin{aligned} \frac{d}{dt}\mathbf{u}(t) &= \mathbf{R}(\mathbf{u}(t), \mathbf{v}(t)) \\ \mathbf{0} &= \mathbf{S}(\mathbf{u}(t), \mathbf{v}(t)) \end{aligned} \tag{22}$$

where $\mathbf{u}(t) = \{P_1\ P_4\ h_2\ h_3\}^T, \mathbf{v}(t) = \{\bar{\rho}_2\ Q_g\ Q_{2-3}\ Q_{4-1}\ V_{V_0}\ V_{v_3}\}^T$, the lines of vector $\mathbf{R}(\mathbf{u}(t), \mathbf{v}(t))$ corresponds to the right hand side of Eqs. (19), (20), (21) and (4), and the lines of vector $\mathbf{S}(\mathbf{u}(t), \mathbf{v}(t))$ corresponds to the algrabraic Eqs. (3), (6), (8), (11), (13) and (14). The condition for this DAE system to have differential index is just

$$\det \frac{\partial \mathbf{S}}{\partial \mathbf{v}}(\mathbf{u}(t), \mathbf{v}(t)) \neq 0. \tag{23}$$

which can be easily checked numerically.

3. Stability Analysis

A system dynamic approach is considered to address the premature shut-off of the fuel supply process. For normal fuel supply process, after the initial transient, there is an almost steady state behaviour. Almost all dependent variables remain constant, except the fuel depth in the fuel tank, which varies linearly with time as is shown in section 3. lbelow. This almost steady state solution (phase II of the normal fuel supply process) can be seen as a stable almost stationary (AS) state. The main hypothesis in this work is that the premature shut-off occurs when the AS state is unstable. To verify this hypothesis the linear stability of the AS state is studied as a function of the system parameters and boundary conditions.

The first step in the linear stability analysis is to construct numerically, as a function of the system parameters and boundary conditions space (SPBC space), the solution corresponding to phase II of the fuel supply process. This solution is denoted as an AS state since it is an explicit linear function of time. The second step is to linearize the governing equations with respect to the AS state. This gives a linear nonautonomous DAE system and standard linear stability techniques do not apply. The finite time (less than the fill up time) action of this linear DAE system over a unitary volume in the phase space dictates the AS state linear stability. If the initially unitary volume contracts with time in all directions (expands in at least one direction) of the phase space, the As state is stable (unstable).

3.1 Almost Stationary State

The AS state is caracterized by constant pressure in the various control volumes composing the fuel tank system (see Fig. 2). The volumetric flow rates Q_{2-3} and Q_{4-1} are also constant. The height h_2 is constant while $h_3 \leq h_f$. When $h_3 > h_f$, the height h_2 becomes a function of time since h_2 has to follow the variation of h_3. In summary, all dependent variables are constant, except h_3 and also h_2 when $h_3 \geq h_f$. Note that when the condition $h_3 > h_f$ is satisfied, there might be a change in the value of the dependent variables. When h_3 is close to reach H, most dependent variables will vary with time and the AS state does not exists anymore. Therefore, the AS state is obtained only for the time interval where the condition $h_3 \leq h_f$ is satisfied. The instant where $h_3 = h_f$ is denoted as t_f, and is a function of the initial condition for variable h_3.

To obtain the AS state in the time interval $[0, t_f]$ (the instant $t = 0$ as the initial instant), the time derivatives in Eqs. (19), (20) and (21) are set to zero. This results in a system of ten algebraic equations since the void fraction α has to be evaluated, and a single ordinary differential equation. The AS state values of variables $P_1,\ P_4,\ h_2,\ \bar{\rho}_2,\ Q_g,\ Q_{2-3},\ Q_{4-1},\ V_{V_0},\ V_{v_3}$ and α is the solution of the algebraic system of non-linear equations

$$\begin{aligned} &\mathbf{R}(P_1,\ P_4,\ h_2,\ \bar{\rho}_2,\ Q_g,\ Q_{2-3},\ Q_{4-1},\ V_{V_0},\ V_{v_3},\ \alpha) = 0 \\ &\mathbf{G}(P_1,\ P_4,\ h_2,\ \bar{\rho}_2,\ Q_g,\ Q_{2-3},\ Q_{4-1},\ V_{V_0},\ V_{v_3},\ \alpha) = 0 \end{aligned} \tag{24}$$

where $\mathbf{R}(P_1,\ P_4,\ h_2,\ \bar{\rho}_2,\ Q_g,\ Q_{2-3},\ Q_{4-1},\ V_{V_0},\ V_{v_3},\ \alpha)$ is the right hand side of the differential part of Eq. (22) and $\mathbf{G}(P_1,\ P_4,\ h_2,\ \bar{\rho}_2,\ Q_g,\ Q_{2-3},\ Q_{4-1},\ V_{V_0},\ V_{v_3},\ \alpha)$ is the algebraic part of Eq. (16). Once the solution $(\tilde{\mathbf{u}}, \tilde{\mathbf{v}}, \alpha)$ of Eq. (24) is obtained, Eq. (4) can be inegrated to obtain

$$h_3(t) - h_3(0) = \frac{(1-\alpha)\tilde{Q}_{2-3}}{A_3} t \tag{25}$$

If h_3 is set equal to h_f in Eq. (25), the result is

$$t_f = \frac{A_3}{(1-\alpha)\tilde{Q}_{2-3}}(h_f - h_3(0)). \tag{26}$$

The AS state obtained above is denoted as $\tilde{\mathbf{x}}^T(t) = \{\tilde{\mathbf{u}}^T(t)\ \tilde{\mathbf{v}}^T(t)\ \alpha\}$ and exists only for the time interval $[0, t_f]$ with t_f given by the Eq. (26).

3.2 Perturbation Governing Equations

The governing equations for the two-phase flow in the fuel tank system are linearized with respect to the AS state. The dependent variables are written as the AS state value plus a infinitesimal perturbation. In other words,

$$\mathbf{x}(t) = \tilde{\mathbf{x}}(t) + \bar{\mathbf{w}}(t), \tag{27}$$

where $\bar{\mathbf{w}}(t) = \{\bar{\mathbf{u}}^T(t)\ \bar{\mathbf{v}}^T(t)\}$ represents the dependent variables infinitesimal perturbations. Eq. (27) is substituted in the Eq. (22). The resulting DAE system is linearized with respect to $\bar{\mathbf{w}}(t)$ since $|\bar{\mathbf{w}}(t)| << 1$ (infinitesimal pertubations), which leads to a linear nonautonomous DAE system given by the Eq.

$$\begin{aligned} \frac{d}{dt}\bar{\mathbf{u}}(t) &= \left[\frac{\partial \mathbf{R}}{\partial \mathbf{u}}(\tilde{\mathbf{u}}(t), \tilde{\mathbf{v}}(t))\right]\bar{\mathbf{u}}(t) + \left[\frac{\partial \mathbf{R}}{\partial \mathbf{v}}(\tilde{\mathbf{u}}(t), \tilde{\mathbf{v}}(t))\right]\bar{\mathbf{v}}(t) \\ \mathbf{0} &= \left[\frac{\partial \mathbf{S}}{\partial \mathbf{u}}(\tilde{\mathbf{u}}(t), \tilde{\mathbf{v}}(t))\right]\bar{\mathbf{u}}(t) + \left[\frac{\partial \mathbf{S}}{\partial \mathbf{v}}(\tilde{\mathbf{u}}(t), \tilde{\mathbf{v}}(t))\right]\bar{\mathbf{v}}(t) \end{aligned} \tag{28}$$

It is assumed that the condition represented by Eq. (23) holds along the AS state $\tilde{\mathbf{x}}(t)$, which implies that the inverse of $[(\partial \mathbf{S}/\partial \mathbf{v})(\tilde{\mathbf{u}}(t), \tilde{\mathbf{v}}(t))]$ exists and Eq. (28) can be reduced to

$$\frac{d}{dt}\bar{\mathbf{u}}(t) = \underbrace{\left(\left[\frac{\partial \mathbf{R}}{\partial \mathbf{u}}(\tilde{\mathbf{u}}(t), \tilde{\mathbf{v}}(t))\right] - \left[\frac{\partial \mathbf{R}}{\partial \mathbf{v}}(\tilde{\mathbf{u}}(t), \tilde{\mathbf{v}}(t))\right]\left[\frac{\partial \mathbf{S}}{\partial \mathbf{v}}(\tilde{\mathbf{u}}(t), \tilde{\mathbf{v}}(t))\right]^{-1}\left[\frac{\partial \mathbf{S}}{\partial \mathbf{u}}(\tilde{\mathbf{u}}(t), \tilde{\mathbf{v}}(t))\right]\right)}_{\mathbf{H}(t)}\bar{\mathbf{u}}(t), \tag{29}$$

which is the AS state perturbation governing equations to be used in the linear stability analysis of the AS state.

3.3 Solution and Stability Criteria

To determine the linear stability of the AS state it is necessary to study the behaviour of the solution of the nonautonomous linear differential equation

$$\frac{d}{dt}\bar{\mathbf{u}}(t) = \mathbf{H}(t)\bar{\mathbf{u}}(t) \tag{30}$$

in the time interval $[0, t_f]$. A unitary volume in the phase space is given as initial conditions. Consider the set $\eta_j = \{0 \ldots \delta_{ij} \ldots\}^T,\ j = 1, \ldots, 4$ of four unitary vectors mutually ortogonal in the phase space as initial conditions for Eq. (30). Let $\varphi_j(t)$ be the solution of Eq. (30) with initial condition η_j. Then, the set $\varphi_j(t),\ j = 1, \ldots, 4$ is a fundamental set of solutions for the ordinary differential equation (ODE) given by Eq. (30). The Wronskian of this set of solutions, given by the equation

$$W(t) = |\varphi_1(t) \ldots \varphi_4(t)|, \tag{31}$$

satisfies the ODE

$$\frac{d}{dt}W(t) = \text{tr}\ \mathbf{H}(t)W(t), \tag{32}$$

where $\text{tr}\ \mathbf{H}(t)$ means the trace of matrix $\mathbf{H}(t)$. This ODE has solution

$$W(t) = \exp(\int_0^t \text{tr}\ \mathbf{H}(\tau)d\tau)W(0). \tag{33}$$

The Wronskian at the initial time $W(0) = |\eta_1 \dots \eta_4| = 1$, represents the volume of the four unitary vector $\eta_j,\ j = 1, \dots, 4$. Therefore, the Wronskian $W(t)$ represents the evolution in time of the unitary volume defined by the four unitary vectors $\eta_j,\ j = 1, \dots, 4$ under the flow generated by the ODE given by Eq. (30). Then $W(t_f) > 1$ represents an expansion of the initial unitary volume in phase space. This implies that there are orbits being repelled from the AS state. As a consequence, the AS state is unstable. If $W(t_f) < 1$ the unitary volume defined by the four unitary vectros $\eta_j,\ j = 1, \dots, 4$ suffered a contraction, but it is not possible to guarantee that the contraction happened in all directions. For example, in one direction there might be an expansion, but in another direction there might be a stronger contraction, and the net result is a volume contraction under the flow generated by the ODE given by Eq. (30) and it is not possible to say that the AS state is stable. To guarantee contraction in all directions and the AS state stability, let $\mathbf{A}$ be the matrix which represents the transformation of the unitary volume defined by the vectors $\eta_j,\ j = 1, \dots, 4$ into the vectors $\varphi_j(t),\ j = 1, \dots, 4$. Then, it follows that

$$[\varphi_1(t_f) \dots \varphi_4(t_f)] = \mathbf{A}\,[\eta_1 \dots \eta_4]\,,$$

and due to the fact that matrix $[\eta_1 \dots \eta_4]$ is the identity matrix, $\mathbf{A}$ is given by the equation

$$\mathbf{A} = [\varphi_1(t_f) \dots \varphi_4(t_f)]\,. \tag{34}$$

If the eigenvalues $\lambda_j, j = 1, \dots, 4$ of matrix $\mathbf{A}$, given by Eq. (34), lie inside the unit circle or $|\lambda_j| \leq 1$ for $j = 1, \dots, 4$, there is no expansion in all directions and the AS state is stable under infinitesimal perturbations.

In summary, the stability criteria is $W(t_f) < 1$ and $|\lambda_j| \leq 1$ for $j = 1, \dots, 4$.

To perform the linear stability analysis of the AS state, $W(t_f)$ has to be evaluated numerically. If $W(t_f) > 1$, the AS state is unstable. If $W(t_f) \leq 1$, the following extra steps has to be performed to determine the stability of the As state:

1. Integrate numerically Eq. (30) in the time interval $[0, t_f]$ under the initial conditions $\bar{\mathbf{u}}(0) = \eta_j, j = 1, \dots, 4$;
2. Compute numericaly the eigenvalues $\lambda_j, j = 1, \dots, 4$ of matrix $\mathbf{A}$.

If $|\lambda_j| \leq 1$ for $j = 1, \dots, 4$, the AS state is stable.

Note that the numerical computation of $W(t_f)$ is faster than the numerical evaluation of the eigenvalues of $\mathbf{A}$ since it involves the numerical integration of Eq. (30) under initial conditions $\bar{\mathbf{u}}(0) = \eta_j, j = 1, \dots, 4$.

4. Results

Part of the results are illustrations of the variation of some dependent variables value at the AS state with respect to variations of the liquid volumetric flow rate Q_l and with respect to variations of the diameter of valve 2 (D_{v_2}). Another result is an illustration of the value of $\int_0^{t_f} \text{tr}\ \mathbf{H}(\tau) d\tau$ with respect to D_{V_2} and Q_l. This result is part of the stability criterion presented above. Positive (negative) values of this quantity implies growth (decay) of the Wronskian and the AS state is unstable (may be stable). The final result is a stability map of the AS state in the $Q_l \times D_{V_2}$ plane.

The parameters value addopted are taken from the reference Fackrell *et al.* (2003). The geometric parameters are as follows: $D_{V_0} = 0.02486\ m, D_1 = 0.0318\ m, D_N = 0.0245\ m, D_{Vt} = 0.0095\ m, A_4 = A_3 = 0.2787\ m^2, h_N = 0.55\ m, h_{ft} = 0.5\ m, h_f = 0.2286\ m, H = 0.315\ m, L_{V_0} = 0.001\ m, L_{V_t} = 0.5\ m, L_{V_2} = 0.05\ m, L_{V_3} = 0.029\ m$ and $L_{V_t} = 0.95\ m$. The working fluids are water and air. The liquid properties are: $\rho_l = 1000\ kg/m^3$ and $\mu_l = 10^{-3}\ Pa/s$. The gas properties are: $\mu_g = 1.81 \times 10^{-5}\ Pa/s$, $R = 287\ J/Kg - K$ and temperature $T = 300K$. The air-water surface tension is $\sigma = 0.073\ N/m$. The atmospheric pressure addopted is $101300\ Pa$. The loss coefficients at the valves are: $K_{exit} = 1.0, K_{ent} = 0.5$ and $K_{reent} = 1.0$. The equivalent lengths are: $Le_1 = 50$ and $Le_2 = 20$. The effect of valve 2 diameter on the AS state stability is studied numerically. Four values of D_{V_2} are considered, and they are: $0.0025\ m,\ 0.0032\ m,\ 0.0064\ m$ and $0.0095\ m$. The loss K_L is a function of valve 2 diameter. For $D_{V_2} = 0.0025\ m$ and $0.0032\ m, K_L = 0.3$. For $D_{V_2} = 0.0064\ m, K_L = 0.8$ and for $D_{V_2} = 0.0095\ m, K_L = 0$.

For all results displayed in Figs. 3 to 7, the range of the liquid volumetric flow rate is $20\ l/min \leq Q_l \leq 60\ l/min$. Figure 3, part (a) and (b), respectively, illustrate the error in the evaluation of the AS state and the manometric pressure at CV0 for the four values of D_{V_2} mentioned above and as a function of Q_l. Figure 4, part (a) and (b) illustrate the manometric pressure at CV4 and the height h_2, respectively, for the four values of D_{V_2} mentioned above and as a function of Q_l. Figure 5 parts (a) and (b) illustrate, respectively, the gas flow rate Q_g into the tank and the gas velocity at the rollover valve for the four values of D_{v_2} mentioned above and as a function of Q_l. Figure 6 parts (a) and (b) illustrate, respectivelly, the void fraction α at the CV2 and the time for the depth h_3 to reach the height h_f for an empty tank ($h_3(0) = 0\ m$) for the four values of D_{V_2} mentioned above and as function of Q_l. Part (a) of Fig. 7 illustrate the value of $\int_0^{t_f} \text{tr}\ \mathbf{H}(\tau) d\tau$ for the four values of D_{V_2} mentioned above and as function of Q_l. Part (b) of Fig. 7 is a stability map of the As state in the $Q_l \times D_{V_2}$ plane.

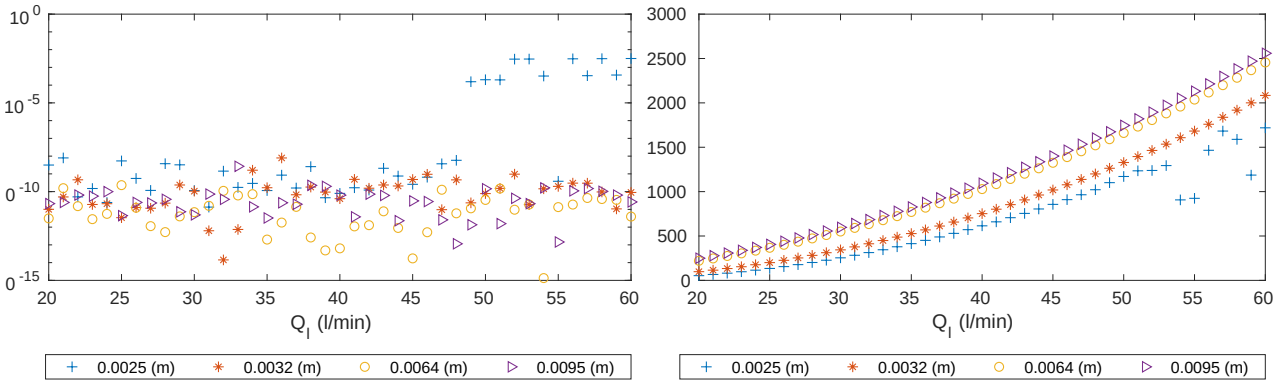

(a) error (b) P_1 (Pa)

Figure 3: Part (a): AS state evaluation error. Part (b): gas pressure in CV0.

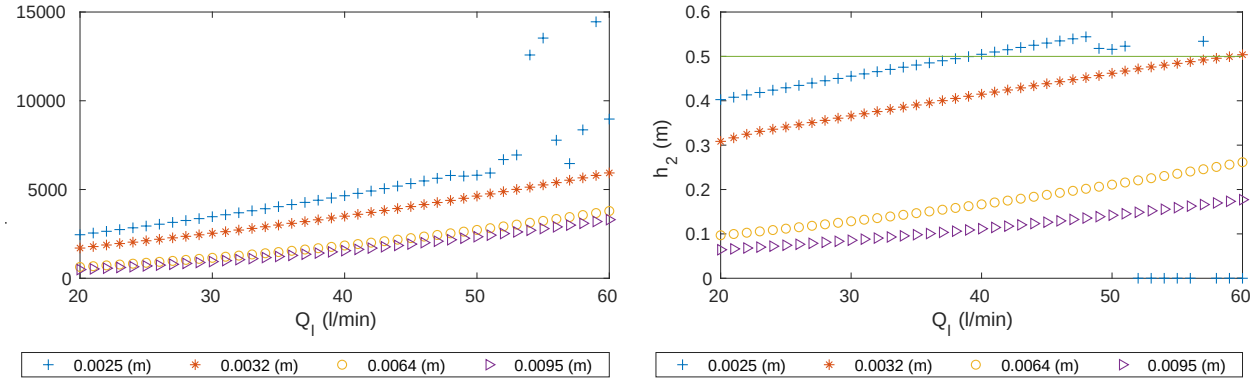

(a) $P_4(Pa)$ (b) h_2 (m)

Figure 4: Part (a): gas tank pressure. Part (b): CV2 height.

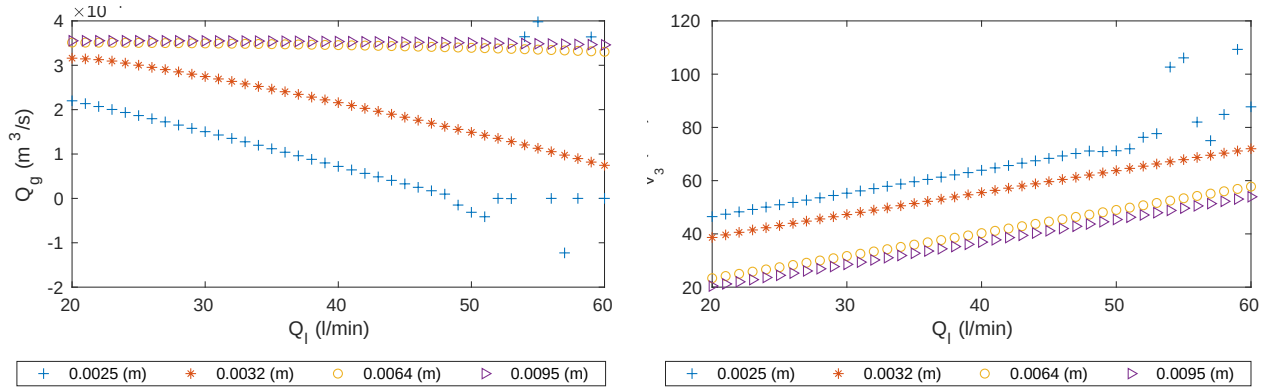

(a) Q_g (m^3/s) (b) V_{3_V}

Figure 5: Part (a): gas volumetric flow rate into the tank. Part (b): gas velocity at the rollover valve.

5. Conclusions and Future Work

According to part (a) of Fig. 7, the time trace time integral is always negative. Therefore, a unitary volume convected by the vector field in a neighbourhood of the AS state contracts, which suggest stability of the AS state for all combinations (Q_l, D_{V_2}) analyzed, and part (b) of Fig. 7 corroborate that the AS state is stable for all pairs (Q_l, D_{V_2}) analyzed. Despite stability of the AS state, there is always an eigenvalue of the matrix $\mathbf{A}$ which lies in the unit circle. In other words,

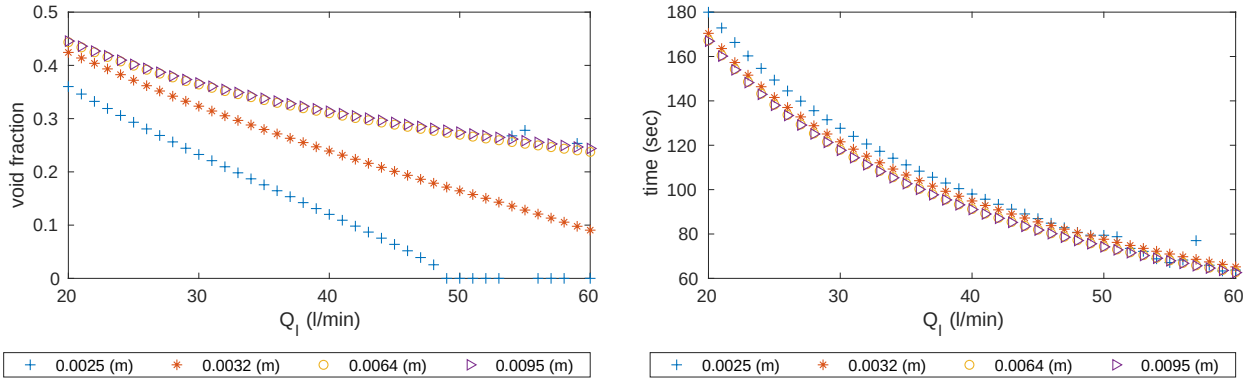

(a) α (b) t_f (sec)

Figure 6: Part (a): void fraction at CV2. Part (b): time for h_3 to reach h_f for $h_3(0) = 0$.

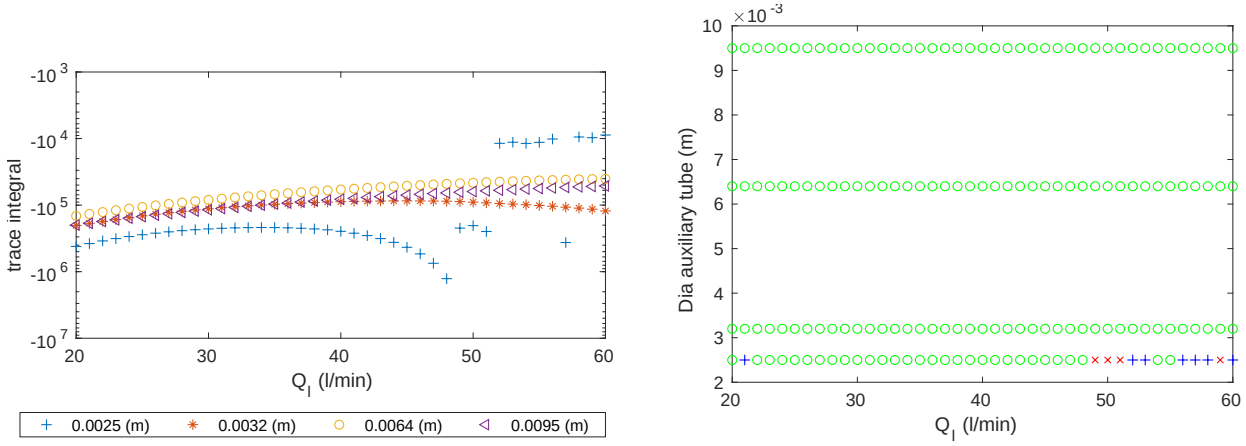

(a) trace intgeral (b) Stability map

Figure 7: Partb(a): trace time integral. Part (b): stability map. $+$: stable, $\times$: unstable and $\circ$: stable but with at least one eigenvalue in the unit circle.

there is always a direction without atraction or repulsion. The only exceptions are the points with $Q_l > 50\ l/min$ and $D_{V_2} = 0.0025\ m$, where acoording to part (a) of Fig. 3 poor convergence of the root search algorithm to determine the AS state is observed. Actually, at those (Q_l, D_{V_2}) pairs the search algorithm was not able to find a solution. According to Fig. 5, for $D_{V_2} = 0.0025\ m$, as $Q_l \to 50\ l/min$, $Q_g \to 0\ m^3/sec$ and $\alpha \to 0$. In the neighborhood of $Q_l = 50\ l/min$, the two-phase flow in CV2 may becomes counter-current ($Q_g < 0$) for a small variation of the volumetric liquid flow rate Q_l, but for a larger increase flooding sets in and the counter-currentn flow is not possible. The AS state for these pairs of (Q_l, D_{V_2}) is not physicaly possible since $h_2 > h_{ft}$ according to part (b) of Fig. 4. During the initial transient, h_2 would reach h_{ft} which stops the fuel pump and no AS state will follow. For these (Q_l, D_{V_2}) pairs premature shutt-off or even a spill back may happen.

The linear stability analysis of the AS state was not able to predict the region in the (Q_l, D_{V_2}) plane were shutt off may occur, but part (b) of Fig. 4 suggest that (Q_l, D_{V_2}) pairs with h_2 close (above) to h_{ft} should not be (are not) physicaly possible and premature shut off or even spill back probably happens. The present results suggest that it is necessary to simulate numerically Eq. (22) to obtain the regions in the SPBC space where premature shut-off happens.

The present model has an improvement with respect to the model presented in Fackrell *et al.* (2003) since in the present work the void fraction is determined by a drift-flux model according to the gas-liquid flow conditions. In Fackrell *et al.* (2003) the void fraction is a parameter and is kept fixed during the mumerical model simulations. The Chexal-Lellouche correlation was chosen since it can handle counter-current flow which was assumed possible to happen at CV2, but according to the present results counter-current flow seldom happens. The choice of the drift flux parameters correlation also limited the working fluids to air and water. The present model lacks important features of the fuel supply process which are the fuel vaporization in the fuel tank and its consequences, like the possibility of chocking at valves 2 and 3 due

to the lower values of sound speed for the air-vapour fuel mixture present in the tank.

This is a report of work in progress. Fuel vaporization effects will be incorporated in future versions of the present model.

6. REFERENCES

Banerjee, R., Bai, X., Pugh, D., Isaac, K.M., Klein, D., Edson, J., Breig, W. and Oliver, L., 2002. "Cfd simulations of critical components in fuel filling systems". In *SAE Technical Paper*. SAE International. doi:10.4271/2002-01-0573. URL https://doi.org/10.4271/2002-01-0573.

Banerjee, R., Isaac, K.M., Oliver, L. and Breig, W., 2001. "A numerical study of automotive gas tank filler pipe two phase flow". In *SAE Technical Paper*. SAE International. doi:10.4271/2001-01-0732. URL https://doi.org/10.4271/2001-01-0732.

Buscariolo, F.F., Magazoni, F., Volpe, L.J.D., Maruyama, F. and Alves, J.C.L., 2015. "Multiphase fuel filling simulation methodology to evaluate different filler neck designs". In *SAE Technical Paper*. SAE International. doi:10.4271/2015-36-0297. URL https://doi.org/10.4271/2015-36-0297.

Chexal, B., Lellouche, G., Horowitz, J. and Healzer, J., 1992. "A void fraction correlation for generalized applications". *Progress in nuclear energy*, Vol. 27, No. 4, pp. 255–295. ISSN 0149-1970. doi:https://doi.org/10.1016/0149-1970(92)90007-P. URL http://www.sciencedirect.com/science/article/pii/014919709290007P.

Chexal, B., Merilo, M., Maulbetsch, J., Horowitz, J., Harrison, J., Westacott, J., Peterson, C., Kastner, W. and Schmidt, H., 1997. "Void fraction technology for design and analysis". Technical report, Electric Power Research Institute., Palo Alto, California.

Dutra, D.G.W., Antônio, S.J. and Eduardo, S.M., 2011. "Automotive cfd fuel tank filling analysis". In *Proceedings of 21st Brazilian Congress of Mechanical Engineering -COBEM 2011*. ABCM.

Fackrell, S., Mastroianni, M. and Rankin, G., 2003. "Model of the filling of an automotive fuel tank". *Mathematical and computer modelling*, Vol. 38, No. 5-6, pp. 519–532.

Godbille, A., Bayliss, M.T. and Pierson, S., 2007. "A parametric vehicle fuel tank filling system model". In *SAE Technical Paper*. SAE International. doi:10.4271/2007-01-1741. URL https://doi.org/10.4271/2007-01-1741.

Govier, G. W.and Aziz, K., 2008. *The Flow of Complex Mixtures in Pipes*. Society of Petroleum Engineers, 2nd edition.

Hibiki, T., 2019. "One-dimensional drift-flux correlations for two-phase flow in medium-size channels". *Experimental and Computational Multiphase Flow*, Vol. 01, No. 02, pp. 85 – 100. ISSN 2661-8877. doi:10.1007/s42757-019-0009-y. URL https://doi.org/10.1007/s42757-019-0009-y.

Lokanathan, M. and Hibiki, T., 2018. "Flow regime transition criteria for co-current downward two-phase flow". *Progress in Nuclear Energy*, Vol. 103, pp. 165–175.

Mastroianni, M., Savoni, L., Henshaw, P. and Rankin, G.W., 2011. "Experimental study of fuel tank filling". *International Journal of Mechanical and Mechatronics Engineering*, Vol. 5, No. 10, pp. 1998 – 2005. ISSN eISSN: 1307-6892. URL https://publications.waset.org/vol/58.

Sinha, N., Thompson, R. and Harrigan, M., 1998. "Computational simulation of fuel shut-off during refueling". In *SAE Technical Paper*. SAE International. doi:10.4271/981377. URL https://doi.org/10.4271/981377.

7. RESPONSIBILITY NOTICE

The author(s) is (are) solely responsible for the printed material included in this paper.